

Article

Effects of Nitrate Assimilation in Leaves and Roots on Biomass Allocation and Drought Stress Responses in Poplar Seedlings

Weifeng Wang^{1,2,*} , Jiazhou Shang^{1,3}, Anders Ræbild² , Tianhui Gao^{1,3} and Qihao Xie¹

¹ College of Forestry, Shanxi Agricultural University, Jinzhong 030801, China; shangjz1111@163.com (J.S.); gaoth1996@163.com (T.G.); xieqihao2022@163.com (Q.X.)

² Department of Geosciences and Natural Resource Management, University of Copenhagen, DK-1958 Frederiksberg C, Denmark; are@ign.ku.dk

³ College of Forestry, Co-Innovation Center for Sustainable Forestry in Southern China, Nanjing Forestry University, Nanjing 210037, China

* Correspondence: wfwang@sxau.edu.cn; Tel.: +86-18203541862

Abstract: Knowledge of tree biomass allocation is fundamental for estimating forest acclimation and carbon stock for global changes in the future. Optimal partitioning theory (OPT) and allometric partitioning theory (APT) are two major patterns of biomass allocation, and occurrences have been tested on taxonomical, ontogenetic, geographic and environmental scales, showing conflicting results and unclear ecophysiological mechanisms. Here, we examine the biomass allocation patterns of two young poplar (*Populus*) clones varying greatly in drought resistance under different soil water and nitrogen availabilities and the major physiological processes involved in biomass partitioning. We found that Biyu, a drought-sensitive hybrid poplar clone, had significant relations among biomass of leaf, stem and root, showing allometric partitioning. Xiaoye, a drought-tolerant poplar clone native to semi-arid areas, on the contrary, showed tightly regulated biomass allocation following optimal partitioning theory. Biyu had higher nitrate reductase activity in the fine roots, while Xiaoye had higher nitrate reductase activity in the leaves. Biochemical analyses and measurements of fluorescence and gas exchange showed that Xiaoye maintained more stable chloroplast membranes and photosystem electron flow, showing higher water use efficiency and a higher resistance to drought. A nitrogen addition could improve leaf photosynthesis and growth both in Biyu and Xiaoye seedlings under drought conditions. We concluded that the two poplar clones showed different biomass allocation patterns and suggest that the site of nitrate assimilation may play a role in biomass partitioning under varying water and nitrogen availabilities.

Keywords: biomass partitioning; poplar; nitrate assimilation; water availability; nitrogen availability



Citation: Wang, W.; Shang, J.; Ræbild, A.; Gao, T.; Xie, Q. Effects of Nitrate Assimilation in Leaves and Roots on Biomass Allocation and Drought Stress Responses in Poplar Seedlings. *Forests* **2024**, *15*, 779. <https://doi.org/10.3390/f15050779>

Academic Editor: Romà Ogaya

Received: 2 April 2024
Revised: 25 April 2024
Accepted: 27 April 2024
Published: 29 April 2024



Copyright: © 2024 by the authors. Licensee MDPI, Basel, Switzerland. This article is an open access article distributed under the terms and conditions of the Creative Commons Attribution (CC BY) license (<https://creativecommons.org/licenses/by/4.0/>).

1. Introduction

Allocation of biomass to organs is essential for plants' acclimation to changing environments. Biomass partitioning among the leaves, stems and roots in trees influences how trees adapt to environmental conditions and is fundamental for predictions of forest carbon stock in response to global changes. Factors such as the availability of light, soil water and nutrients; mycorrhiza; and plants' ontogenetic development can affect the carbohydrate allocation fractions to leaves, stems and roots [1,2]. Optimal partitioning theory (OPT) and allometric partitioning theory (APT) are the two main theories proposed to explain the biomass allocation patterns among plant species facing different environments [3].

Biomass partitioning to organs is sometimes seen as a result of plastic responses of organs to environmental variation [1], limited by the genetics of the species. For many crops and tree species, the root/shoot ratio is high if the nitrogen concentration is kept at low levels, but above a critical point, it would decrease with increasing nitrogen levels [4]. A recent meta-analysis of terrestrial plants at the global scale showed that nitrogen addition increased leaf, stem and shoot mass fractions by an average of 13%, while the root/shoot

ratio and root mass fraction declined by 27% and 15%, respectively [5]. These results suggested that plants need to partition more biomass to roots to take up nutrients when soils are poor, but that plants benefit from partitioning more biomass to shoots to capture light when the soil is at a high nutrition level. Trees also extend their root systems and get higher root/shoot ratios during soil drought to improve potentials for water uptake [6]. According to OPT, biomass should be allocated to the organ which can obtain the most limiting resource for the whole plant in order to maximize the relative growth rate [7]. This relates to the concept of “functional equilibrium”, which means that plants will allocate relatively more biomass to roots when belowground factors (e.g., nutrients and water) are limiting, while they allocate relatively more biomass to shoots when aboveground factors (e.g., light) are limiting [2].

However, some plants show rather stable allometric partitioning among compartments [8,9]. This resulted in the development of APT, which is based on a general allometric equation, $\log Y = \log \beta + \alpha \log X$, where Y and X mean the biomass of vegetative organs, emphasizing that biomass partitioning among organs is dependent more on plant size and less on environmental factors [10]. The parameter β is an allometric constant, and α is a scaling exponent which reflects the relative growth rate ratio between organs X and Y . Allometric analyses of many taxa, including lianas, conifers and angiosperm trees, supported APT [3,11,12]. Furthermore, by using a global database, Poorter et al. [13] found that the scaling exponent in plants is dependent on ontogeny, and that annual plants or juvenile trees had a higher leaf biomass fraction than adult trees. Though the allocation of biomass accumulated over several years follows APT, the limiting resource or factor in each year may change with ontogeny [12], meaning that the annual biomass allocation may still be impacted by environment factors. The physiological mechanisms that control the partitioning of photoassimilates are key to plant growth, and the levels of soluble sugars and nitrate are important [2]. However, these mechanisms are still unclear [14]. Based on an analysis of different shade- and drought-tolerant trees, Puglielli et al. [15] proposed that plant function type determines the biomass allocation patterns and that plant biomass allocation strategies are based on the interactions of functional type, ontogeny and species-specific stress-tolerance adaptations.

In this study, a drought-sensitive hybrid poplar clone (Biyu, a bud mutation of the male clone *Populus deltoides* ‘2025’, which was bred from *Populus deltoides* ‘Lux’ \times *P. deltoides*) [16] and a drought tolerant poplar clone (Xiaoye, *P. simonii*) native to semi-arid areas of Northern China [17] were grown under controlled soil water and nitrogen availabilities. *P. deltoides*, the parent species of Biyu, is frequently applied in poplar breeding and is ecologically important in the riparian ecosystem in its native range, from the Southeastern United States to Southern Canada [18]. *P. simonii* is widely distributed in Northern China and possesses drought and cold tolerance, allowing it to grow well under many edaphic and climatic conditions [19]. However, knowledge on biomass allocation patterns among poplar species with different drought tolerance and their underlying ecophysiological mechanisms is still lacking. We aimed to (1) distinguish whether the two clones have different biomass allocation patterns under different soil water and nitrogen availabilities and (2) explore the key processes in carbon and nitrogen metabolism and their relationships with biomass allocation patterns.

2. Materials and Methods

2.1. Plant Materials and Treatments

A hybrid poplar clone Biyu (a bud mutation from a widely planted hybrid clone 2025, *P. deltoides* 'Lux' × *P. deltoides*, drought sensitive) and a species clone Xiaoye (native to semi-arid areas of Northern China, *P. simonii*, drought tolerant) were used for this study. Poplar clones were propagated from 15 cm long cuttings cut from one-year-old stems. Air-dried and sieved native brown sandy loam soil was used with 15 kg in each 19 L plastic pot. Soil field capacity was 26.9%, with a pH of 8.3, organic content of 14.6 g kg⁻¹, total salt of 0.1%, total nitrogen of 1.1 g kg⁻¹, available nitrogen of 48.8 mg kg⁻¹, available phosphorus of 9.6 mg kg⁻¹ and available potassium of 123.3 mg kg⁻¹. A layer of 2–3 cm size pebbles was placed in the bottom of each pot and separated from the soil by a piece of 300 mesh nylon. Water could get into the stones through a 1.2 cm PVC tube and then wet the soil. All cuttings were planted in pots with pre-watered soil on 1 April 2021, with one cutting in each pot. Pots were placed under a polycarbonate transparent shelter, situated in the forest experimental station of Shanxi Agricultural University (37°25' N, 112°34' E, 796 m elevation), Taigu District, Jinzhong City, Shanxi Province, China. The station is located in the eastern part of the Loss Plateau, and the mean annual air temperature, total precipitation, evaporation capacity and sunshine hours are 10.4 °C, 397.1 mm, 1649 mm and 2527.5 h, respectively. Each pot was weighed and watered daily to 80 ± 5% of field capacity, corresponding to a water potential of -0.018 ± 0.002 MPa measured with a soil tensiometer.

All pots were watered regularly and weeded until the seedlings, after three months, were about 60 cm high with 9–10 leaves. Forty pots of each clone were randomly assigned on 1 July 2021, and four treatments were established: control (CK, 80 ± 5% of field capacity and 0 g NH₄NO₃ plant⁻¹); drought (D, 40 ± 5% of field capacity, corresponding to a water potential of -0.047 ± 0.003 MPa and a mild drought stress, and 0 g NH₄NO₃ plant⁻¹); nitrogen addition (NA, 80 ± 5% of field capacity and 6 g NH₄NO₃ plant⁻¹); and drought and nitrogen addition (D + NA, 40 ± 5% of field capacity and 6 g NH₄NO₃ plant⁻¹). The fertilizer treatment included an addition of 6 g NH₄NO₃ per pot, distributed across three times, respectively, on 1 July, 11 July and 21 July 2021, with 2 g each time. NH₄NO₃ was dissolved in water and added to pots during watering. Plants were placed randomly under the shelter, and the positions of pots were changed at the end of July and at the end of August to minimize the influences of possible variation in environmental factors. The following ecophysiological parameters were measured when seedlings had 30–35 leaves.

2.2. Gas Exchange and Chlorophyll Fluorescence Measurements

Measurements of leaf gas exchange were conducted on 21–22 August 2021 by using a portable photosynthetic system (Li-6400XT; LICOR Biosciences, Lincoln, NE, USA). One fully expanded leaf per plant in the upper canopy was measured from 9:00 to 11:30 on calm and clear days, with 6–8 plants per treatment and clone. The conditions in the 2 × 3 cm leaf chamber consisted of a photosynthetic photon flux density (PPFD) of 1500 μmol m⁻² s⁻¹, a leaf temperature of 28 °C, a gas flow rate of 500 μmol s⁻¹ and an air entering CO₂ concentration of 450 μmol mol⁻¹. Then, the leaf net photosynthetic rate at saturated light intensity (A_{sat} , μmol m⁻² s⁻¹) and transpiration rate (E , mmol m⁻² s⁻¹) were measured, and the instantaneous water use efficiency (WUE_i) was calculated as A_{sat}/E . Chlorophyll fluorescence parameters were measured on the same leaves used for gas exchange measurement on 22–23 August with a portable chlorophyll fluorometer (PAM-2500; Heinz Walz GmbH, Effeltrich, Germany), according to Murchie and Lawson [20]. Firstly, the origin (F_0) and maximum fluorescence (F_m) were measured after 30 min in the dark with leaf clips. Then, an artificial actinic light of 278 μmol m⁻² s⁻¹ was applied, and maximum fluorescence in the light-adapted state (F_m') was measured after 3–5 min. The actual photochemical yield of PSII (Φ_{PSII}), non-photochemical quenching (NPQ), coefficient of photochemical quenching (q_p) and electron transport rate (ETR) were recorded [20].

2.3. Chlorophyll Content, Microanatomy, and Nitrogen and Carbon Content

Chlorophyll content and microstructure were measured on 22 August 2021, on leaves adjacent to the ones used for measurements of gas exchange, avoiding main veins. Chlorophyll a and b contents per leaf area were determined with a spectrophotometer after chlorophyll pigments were extracted in darkness with 95% ethanol from small leaf disks of known area [21]. Total chlorophyll content was calculated as the sum of chlorophyll a and b. The middle section (1×1 cm) of the leaf was sampled and fixed in formaldehyde solution (FAA) for microanatomical measurements. After dehydration with a series of ethanol solutions, leaf sections were cleared and embedded in paraffin. Then, $15 \mu\text{m}$ sections were cut with a rotary microtome (RM2235; Leica Biosystems, Wetzlar, Germany) and stained with safranin O and fast green. Sections were observed at $400\times$ magnification, and images captured with a microscope camera (CX31 and DP27, Olympus, Tokyo, Japan). Leaf thickness (LT), palisade tissue thickness (T_{pal}) and spongy tissue thickness (T_{spo}) were determined with ImageJ 1.54g software, and $T_{\text{pal}}/T_{\text{spo}}$ was calculated.

Two fully expanded leaves next to the leaves used for gas exchange of each plant were sampled on 24 August 2021 to determine single leaf area (LA) with a scanner. Leaves were dried at 105°C for 30 min, followed by drying at 75°C until a constant weight and weighed. Leaf samples were ground, and leaf total nitrogen content per unit mass (LN) was determined using the Kjeldahl method [22]. Then, the leaf mass per area (LMA), leaf density (LD, LMA/LT), nitrogen content per leaf area (N_{area}) and photosynthetic nitrogen use efficiency (PNUE, $A_{\text{sat}}/N_{\text{area}}$) were calculated from the above data. Leaf total carbon content per unit mass was analyzed by using an elemental analyzer (multi N/C2100; Analytik Jena, Jena, Germany), and the leaf carbon-to-nitrogen ratio (C/N) was calculated. Leaf stable carbon isotope composition ($\delta^{13}\text{C}$) was determined with a mass spectrometer (Delta V Advantage; Thermo Fisher Scientific, Waltham, MA, USA) with an interface (Conflo III; Finnigan MAT).

2.4. Malondialdehyde (MDA), Nitrate Reductase Activity (NR) and Free Proline

Leaf and fine root fresh samples were collected on 26 August 2021, and immediately submerged in liquid nitrogen before being stored in a -80°C freezer. Leaf MDA content was measured by using the thiobarbituric acid method, according to Hodges et al. [23]. The activities of peroxidases (POD, EC 1.15.1.7) and superoxide dismutase (SOD, EC 1.15.1.1) in leaves were determined according to the kit guides (BC0090 and BC0175, Solarbio, Beijing, China). NR (EC 1.7.99.4) activities in leaves (NR_{leaf}) and in fine roots (NR_{root}) were determined according to the kit guide (BC0085, Solarbio, Beijing, China). The free proline content of dry leaf samples was determined using a spectrophotometer, according to the kit guide (BC0290, Solarbio, Beijing, China).

2.5. Biomass Allocation, Soluble Sugar and Starch

The plants were harvested on 15–17 September 2021. Firstly, the height and base diameter were measured. Leaves and stems were harvested, and whole roots were washed carefully. Coarse roots and fine roots were separated using a 2 mm diameter threshold. Each plant was divided into four parts: leaves, stem, coarse roots and fine roots. They were dried at 105°C for 30 min, followed by drying at 75°C until a constant weight was reached. The dry weight of these parts was determined. Shoot weight was calculated as the sum of leaf and stem weights, root weight was calculated as the sum of coarse root and fine root weights, followed by the calculation of biomass fractions. The content of soluble sugars and starch of ground leaf samples were determined using the phenol-sulfuric acid method, according to Landhäusser et al. [24].

2.6. Statistical Analysis

Statistical tests were performed using R version 4.3.1 [25]. Firstly, the normality of all data was tested using the “*shapiro.test*” function. As the trees were completely randomized, three-way ANOVAs were performed to test the impacts of drought, nitrogen addition, clone and their interactions, using the “*aov*” function. Tukey’s HSD post hoc tests were performed to test for significant differences among the treatments, using the “*TukeyHSD*” function, at $p \leq 0.05$. The assignment of letters to means after pairwise comparisons was conducted using the “*multcompLetters4*” and “*as.data.frame.list*” functions. Standardized major axis analysis was performed in the “*mastr*” package to determine scaling exponents (α), according to Niklas and Enquist [10]. Principal component analysis (PCA) was conducted using “*prcomp*” and “*fviz_pca_biplot*” functions.

3. Results

3.1. Growth and Biomass Allocation Changes under Water and Nitrogen Availabilities

As expected, the plant height, diameter and biomass of the whole plant in both clones were smaller under drought and increased by nitrogen addition. Biyu seedlings under nitrogen addition had the largest total biomass, and both the biomass distribution and fractions were significantly different between clones (Figure 1a; Supplementary Tables S1 and S2). Biyu and Xiaoye were significantly different between clones in both organ biomass distribution and organ biomass fractions, except for total biomass (Figure 1 and Supplementary Table S2). Biyu showed an allometric biomass allocation pattern with significant scaling exponents ranging from 0.98 to 1.13, and R^2 ranging from 0.87 to 0.97 (Figure 2). Meanwhile, allometric relations were insignificant for Xiaoye, except for a significant relation between leaf and stem biomass, with $\alpha = 0.87$ and $R^2 = 0.57$. Moreover, the stem biomass fraction decreased significantly under drought, and the root biomass fraction decreased under nitrogen addition. Hence, Xiaoye showed varying biomass allocation patterns, supporting the idea that this clone follows an optimal biomass partitioning pattern (Figures 1 and 2).

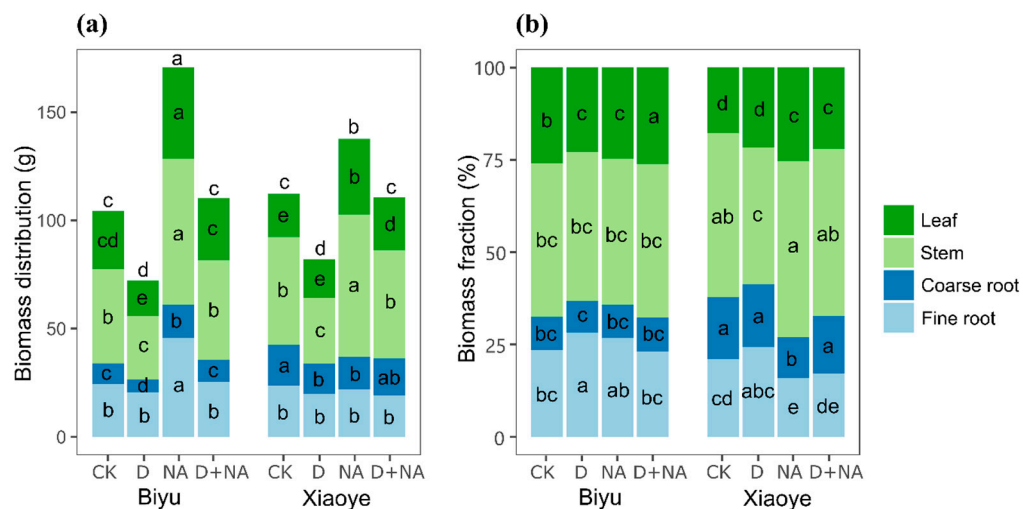


Figure 1. Biomass distribution of leaf, stem, coarse root and fine root in whole plant (a) and their biomass fraction changes (b) in Biyu and Xiaoye seedlings after water and nitrogen treatments. Values shown are means. Different letters indicate statistical differences among treatments (Tukey HSD, $p < 0.05$). The significance levels of the factors and interactions are shown in Supplementary Table S2. Treatments: CK, control; D, drought; NA, nitrogen addition; D + NA, drought and nitrogen addition.

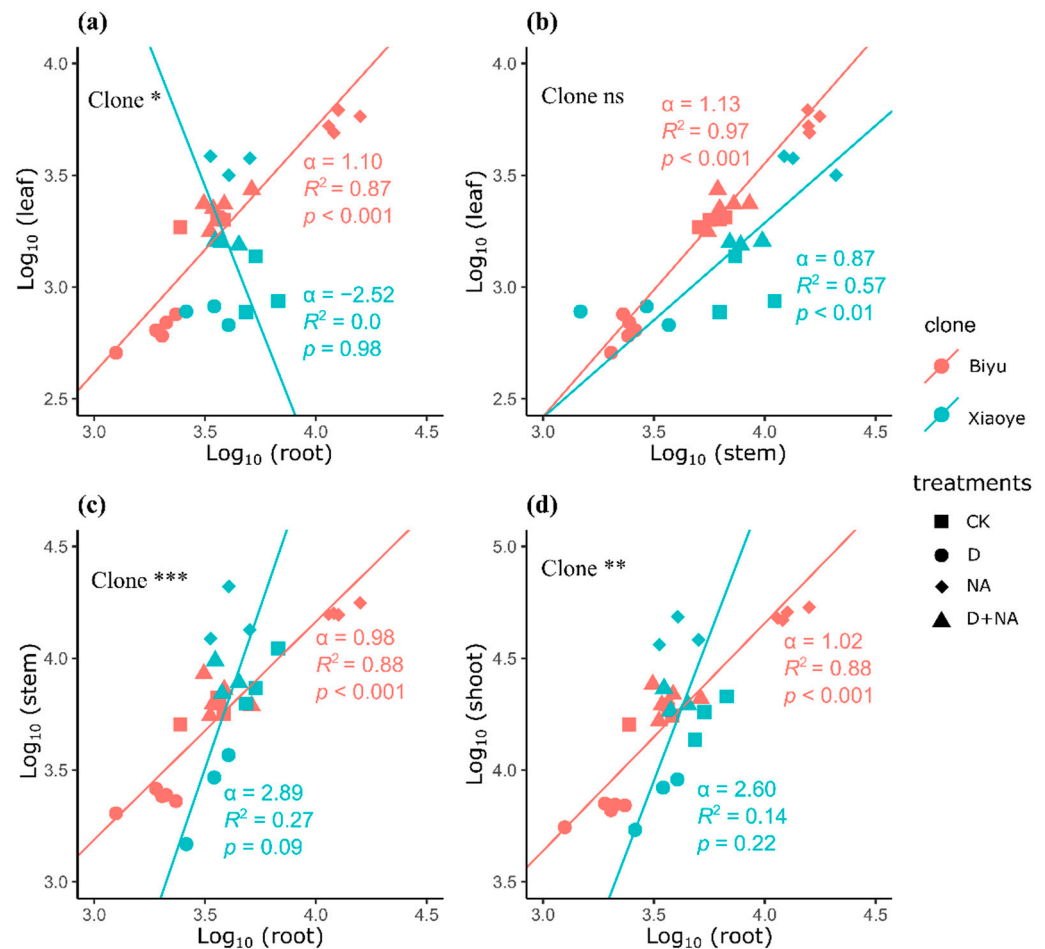


Figure 2. Standard major axis regressions between leaf and root biomass (a), leaf and stem biomass (b), stem and root biomass and (c) shoot and root biomass (d) of Biyu and Xiaoye seedlings. All data are log_{10} transformed. Abbreviations: α , scaling exponent. Treatments: CK, control; D, drought; NA, nitrogen addition; D + NA, drought and nitrogen addition. Clone followed by asterisks indicates significance levels between regressions of the two clones: ns $p > 0.05$, * $0.01 < p < 0.05$, ** $0.001 < p < 0.01$ and *** $p < 0.001$.

3.2. Nitrogen Assimilation and Leaf Nitrogen Status

The NR activity in the leaves of Biyu was significantly lower than that of Xiaoye, but in fine roots, the pattern was the opposite, as NR_{root} was higher in Biyu (Figure 3). The drought and nitrogen addition significantly increased NR_{leaf} in both Biyu and Xiaoye. NR_{root} of Biyu decreased by D and D + NA treatments, but NA treatment alone did not significantly impact NR_{root} in the clones (Figure 3). In both Biyu and Xiaoye seedlings, single leaf area significantly decreased under drought conditions and increased under high nitrogen availability, while the leaf nitrogen content of D treatment did not differ significantly from CK. Nitrogen addition significantly increased leaf nitrogen content. Biyu had a higher leaf area but lower nitrogen content than Xiaoye. In Biyu seedlings, nitrogen addition significantly increased the N_{area} and decreased C/N, while the N_{area} and C/N in Xiaoye did not change. The LMA and leaf density in both Biyu and Xiaoye decreased significantly with the nitrogen addition but showed no differences with drought (Table 1).

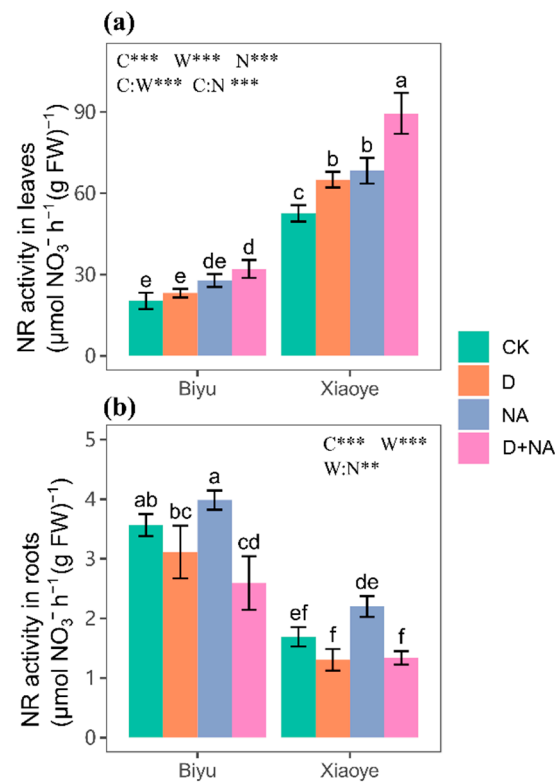


Figure 3. Nitrate reductase activity changes in leaves (a) and fine roots (b) of Biyu and Xiaoye seedlings. Treatments: CK, control; D, drought; NA, nitrogen addition; D + NA, drought and nitrogen addition. Values shown are means \pm SD. Different letters indicate statistical differences among treatments (Tukey HSD, $p < 0.05$). The significance levels of factors and their interactions are indicated as ** $0.001 < p < 0.01$ and *** $p < 0.001$. Abbreviations for factors and their interactions: C, poplar clone; W, water; N, nitrogen; C:W, interaction between clone and water; C:N, interaction between clone and nitrogen; W:N, interaction between water level and nitrogen; C:W:N, interactions among clone, water and nitrogen.

3.3. Leaf Ecophysiological Traits

The leaf MDA of Biyu significantly increased under D treatment, but that of Xiaoye did not change among four treatments (Figure 4a). The activities of POD and SOD in leaves were increased by drought and nitrogen addition, and with slightly larger amounts in Xiaoye compared to Biyu (Supplementary Figure S1). The nitrogen addition significantly increased the total chlorophyll content per leaf area, but drought had no effect (Figure 4b). The $T_{\text{pal}}/T_{\text{spo}}$ ratio was slightly lower in Biyu than in Xiaoye, and the nitrogen addition significantly increased the $T_{\text{pal}}/T_{\text{spo}}$ of Xiaoye (Figure 4c). The Φ_{PSII} of Biyu declined significantly under drought, but the reduction was lower under nitrogen addition. The Φ_{PSII} of Xiaoye did not change (Figure 4d). The NPQ of Biyu increased under drought, and the two clones showed different NPQ changes under the four treatments (Figure 4e). For Biyu seedlings, the q_p and ETR were decreased by the D and D + NA treatments, while these parameters did not change significantly in Xiaoye (Table 1). The A_{sat} of both clones decreased under drought and increased following the nitrogen addition (Figure 4f).

Table 1. Ecophysiological traits of newly grown leaves under drought and/or nitrogen addition treatments for Biyu and Xiaoye seedlings, and results from analyses of variance.

	Biyu				Xiaoye				Results from Analysis of Variance						
	CK	D	NA	D + NA	CK	D	NA	D + NA	C	W	N	C:W	C:N	W:N	C:W:N
LA (cm ²)	151 ± 9 b	69 ± 6 e	178 ± 6 a	117 ± 8 c	124 ± 9 c	64 ± 4 e	159 ± 9 b	87 ± 6 d	***	***	***	0.34	*	0.12	***
LN (mg g ⁻¹)	11.9 ± 0.7 d	12.4 ± 0.6 d	16.8 ± 0.7 bc	19.3 ± 1.3 a	15.0 ± 0.8 c	15.5 ± 0.7 c	18.9 ± 0.9 ab	19.6 ± 0.6 a	***	***	**	0.15	**	0.07	0.18
N _{area} (g m ⁻²)	0.89 ± 0.06 c	0.89 ± 0.04 c	1.05 ± 0.05 b	1.18 ± 0.08 a	0.95 ± 0.05 bc	1.01 ± 0.04 bc	1.04 ± 0.05 b	1.02 ± 0.03 bc	0.95	*	***	0.19	***	0.26	*
C/N	32 ± 5 a	28 ± 3 ab	23 ± 2 ab	20 ± 0.6 b	26 ± 2 ab	24 ± 2 ab	22 ± 10 ab	21 ± 2 b	0.08	0.11	***	0.44	0.14	0.99	0.97
LMA (g m ⁻²)	74.4 ± 3 a	71.5 ± 2 b	62.6 ± 3 d	61.4 ± 3 de	63.6 ± 1 c	64.8 ± 2 b	55.1 ± 3 e	52.1 ± 5 e	***	0.18	***	0.62	0.90	0.76	0.20
LD (g cm ⁻³)	0.30 ± 0.01 a	0.30 ± 0.01 a	0.26 ± 0.02 bc	0.27 ± 0.01 bc	0.29 ± 0.01 ab	0.28 ± 0.01 ab	0.26 ± 0.02 bc	0.24 ± 0.02 c	**	0.18	***	0.15	0.94	0.94	0.75
q _p	0.86 ± 0.02 a	0.71 ± 0.00 c	0.85 ± 0.02 a	0.69 ± 0.01 c	0.81 ± 0.02 b	0.82 ± 0.02 b	0.84 ± 0.03 ab	0.83 ± 0.01 ab	***	***	0.27	***	**	0.24	0.96
ETR (μmol e m ⁻² s ⁻¹)	74 ± 2 a	54 ± 2 c	75 ± 3 a	62 ± 2 b	72 ± 2 a	73 ± 1 a	74 ± 2 a	74 ± 1 a	***	***	***	***	*	*	***
Free Proline (mg g ⁻¹)	42 ± 0.9 d	52 ± 2 bc	40 ± 2 d	51 ± 4 bc	45 ± 3 cd	66 ± 4 a	45 ± 4 cd	54 ± 2 b	***	***	**	0.06	0.06	*	*
PNUE (μmol g ⁻¹ s ⁻¹)	27.4 ± 2 a	23.8 ± 1 b	26.6 ± 1 ab	24.0 ± 2 b	28.4 ± 1 a	23.3 ± 1 b	28.6 ± 1 a	26.5 ± 1 ab	*	***	0.26	0.65	0.07	0.09	0.35
WUE _i (μmol mmol ⁻¹)	3.39 ± 0.26 cd	3.16 ± 0.21 d	3.30 ± 0.22 cd	3.35 ± 0.21 cd	4.32 ± 0.34 a	4.49 ± 0.42 a	4.15 ± 0.18 ab	3.76 ± 0.25 bc	***	0.16	*	0.74	**	0.37	**
δ ¹³ C (%)	-30.5 ± 0.2 cd	-30.8 ± 0.4 d	-30.0 ± 0.4 abc	-29.9 ± 0.4 abc	-30.3 ± 0.3 bcd	-29.9 ± 0.4 abc	-29.3 ± 0.3 ab	-29.3 ± 0.2 a	***	0.84	***	0.27	0.94	0.72	0.14

Note: Values shown are means ± SD. Different letters indicate statistical differences among treatments (Tukey HSD, $p < 0.05$). The p -values (* $0.01 < p < 0.05$, ** $0.001 < p < 0.01$ and *** $p < 0.001$) show the results of ANOVA. Abbreviations of treatments and variables: CK, control treatment; D, drought; NA, nitrogen addition; D + NA, drought and nitrogen addition; LA, single leaf area; LN, leaf nitrogen content per mass; N_{area}, leaf nitrogen content per area; C/N, leaf carbon-to-nitrogen ratio; LMA, leaf mass per area; LD, leaf density; q_p, photochemical quenching; ETR, electron transport rate; PNUE, photosynthetic nitrogen use efficiency; WUE_i, instantaneous water use efficiency; δ¹³C, leaf ¹³C-to-¹²C ratio. Abbreviations for factors and their interactions: C, poplar clone; W, water; N, nitrogen; C:W, interaction between clone and water; C:N, interaction between clone and nitrogen; W:N, interaction between water level and nitrogen; C:W:N, interactions among clone, water and nitrogen.

Xiaoye had higher free proline content than Biyu, and both clones had significantly increased contents under drought (Table 1). The leaf soluble sugar contents of Biyu were significantly higher than in Xiaoye; and both drought and the nitrogen addition increased the soluble sugar contents of Biyu (Figure 5a), while those of Xiaoye were not affected by treatments. The starch content of Xiaoye was higher than that of Biyu, and there was a tendency of higher starch content in the D + NA treatment, which was significant in Xiaoye (Figure 5b). Drought caused a decrease in PNUE in both clones. While WUE_i did not change in Biyu, the D + NA treatment caused a decrease in WUE_i in Xiaoye compared to the control treatment. Moreover, Xiaoye had higher WUE_i and $\delta^{13}C$ than Biyu (Table 1).

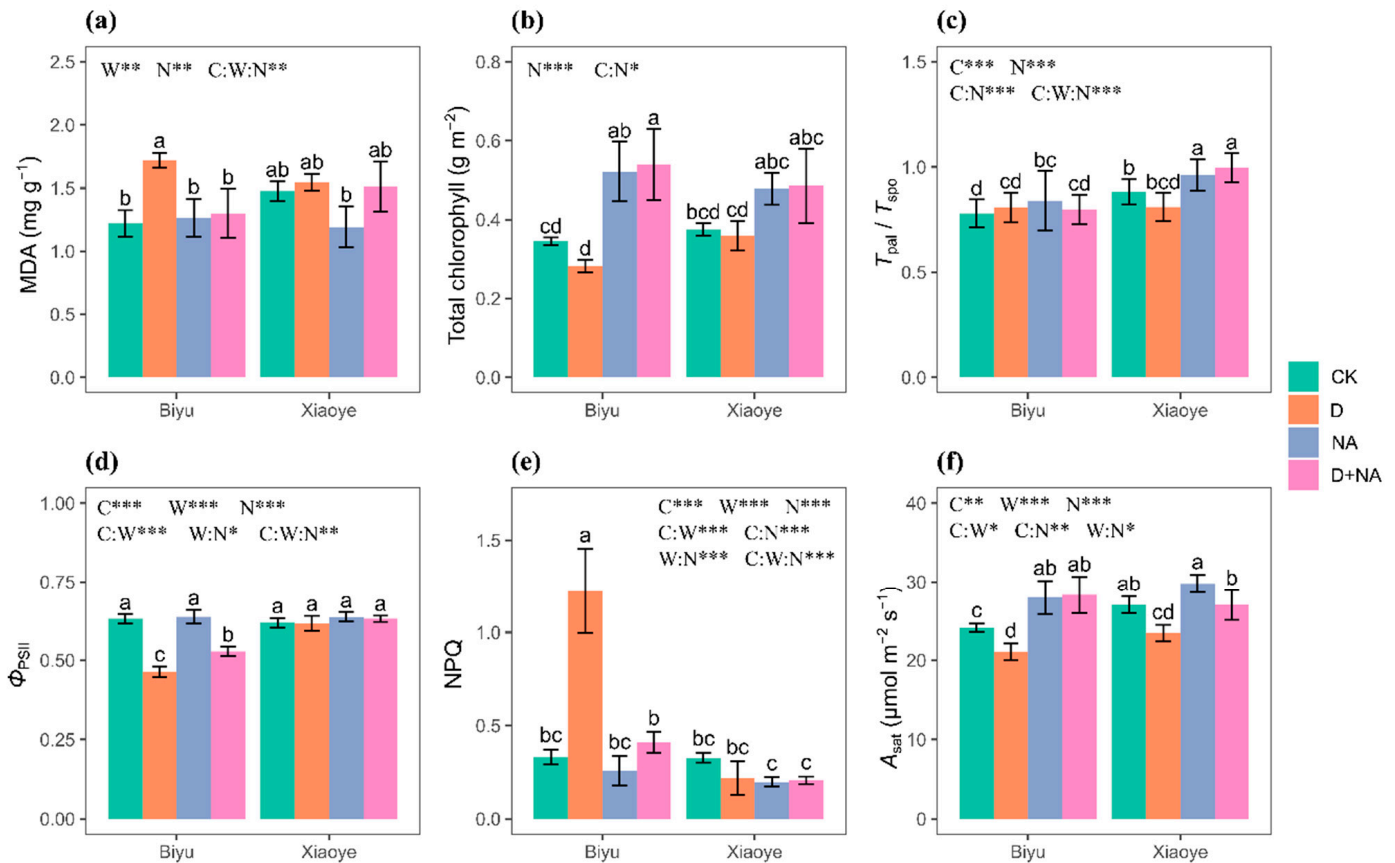


Figure 4. Leaf ecophysiological traits changes in Biyu and Xiaoye. (a) malondialdehyde content (MDA); (b) the sum of chlorophyll a and chlorophyll b; (c) ratio of palisade tissue thickness to spongy tissue thickness (T_{pal}/T_{spo}); (d) actual photochemical yield of PSII (Φ_{PSII}); (e) non-photochemical quenching (NPQ); (f) net photosynthesis rate at saturated light intensity (A_{sat}). Treatments: CK, control; D, drought; NA, nitrogen addition; D + NA, drought and nitrogen addition. Values shown are means \pm SD. Different letters indicate statistical differences among treatments (Tukey HSD, $p < 0.05$). The significance levels of factors are indicated as * $0.01 < p < 0.05$, ** $0.001 < p < 0.01$ and *** $p < 0.001$. For abbreviations of factors, see Figure 3.

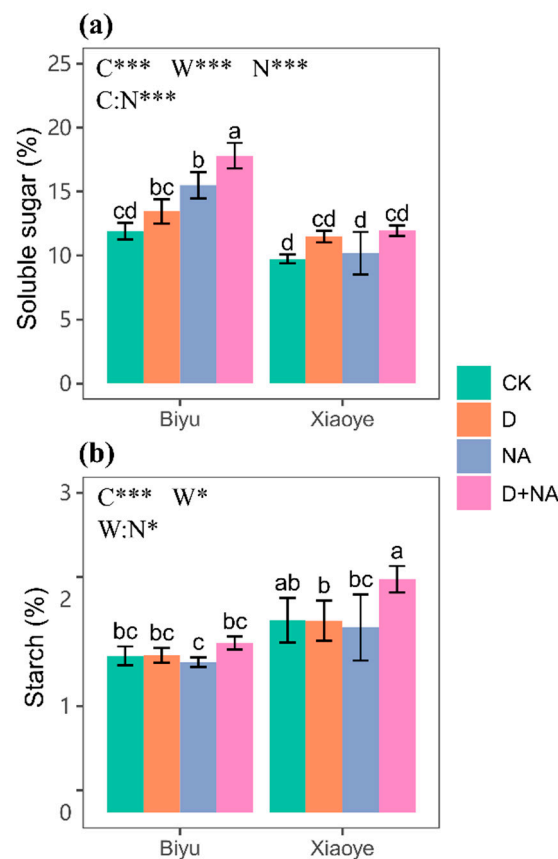


Figure 5. Soluble sugar (a) and starch content (b) changes in leaves. Treatments: CK, control; D, drought; NA, nitrogen addition; D + NA, drought and nitrogen addition. Values shown are means \pm SD. Different letters indicate statistical differences among treatments (Tukey HSD, $p < 0.05$). The significance levels of factors are indicated as * $0.01 < p < 0.05$, and *** $p < 0.001$. For abbreviations of factors, see Figure 3.

3.4. Principal Component Analysis

The results showed that Xiaoye had more stable leaf MDA, Φ_{PSII} , NPQ, q_P and ETR under water and nitrogen availabilities, and it had higher NR_{leaf} , WUE_i and $\delta^{13}C$ than Biyu (Figures 3 and 4; Table 1). A PCA based on ecophysiological traits was used to explore the relations between the measured parameters and the differences between clones under soil water and nitrogen availabilities. Biyu and Xiaoye separated into two obviously different groups (Figure 6). The NR activity in leaves or in fine roots appeared to be the most important traits, inducing differences between the clones. NR_{root} , soluble sugar content and LMA were associated with Biyu, whereas NR_{leaf} , starch content, WUE_i and free proline content were associated with Xiaoye.

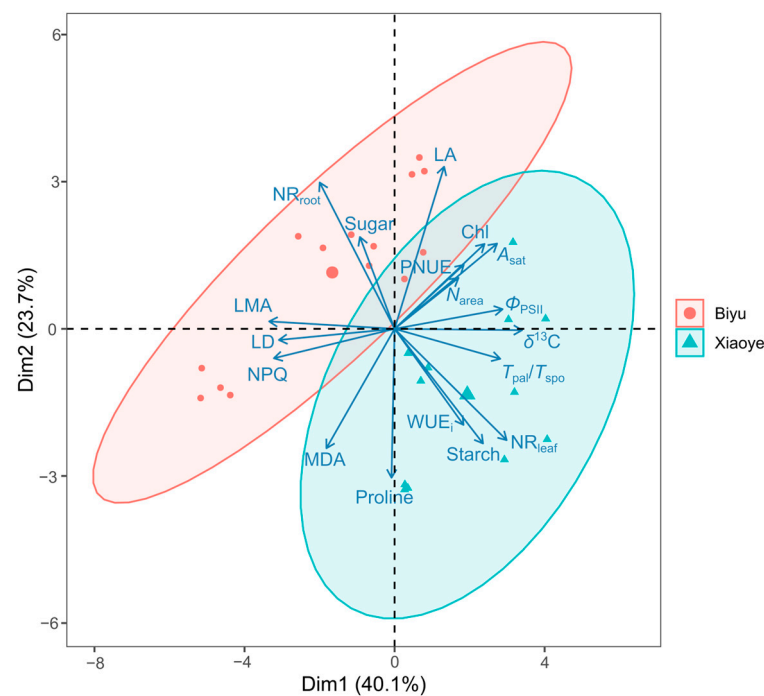


Figure 6. Principal component analysis of ecophysiological traits between Biyu and Xiaoye clones. Abbreviations: LA, single leaf area; LMA, leaf mass per area; Sugar, soluble sugar content; NR_{leaf} , nitrate reductase activity in leaves; NR_{root} , nitrate reductase activity in fine roots; LD, leaf density; MDA, malondialdehyde content; WUE_i , instantaneous water use efficiency; Proline, free proline content; A_{sat} , net photosynthesis rate at saturated light intensity; Chl, total chlorophyll content per leaf area; Sugar, soluble sugar content; Starch, starch content; $\delta^{13}C$, stable carbon isotope composition; T_{pal}/T_{spo} , ratio of palisade tissue thickness to spongy tissue thickness; N_{area} , nitrogen content per leaf area; NPQ, non-photochemical quenching; Φ_{PSII} , quantum yield of photosystem II.

4. Discussion

Biomass allocation to organs plays a very important role in resource acquisition and growth improvement [1]. Both clones showed increased plant height and leaf area in response to high soil water and nitrogen availabilities (Supplementary Table S1 and Table 1). However, the two clones showed different biomass allocation patterns. The native poplar clone Xiaoye had a significantly reduced root fraction and increased leaf fraction under nitrogen addition, and it had a reduced stem fraction and increased root fraction under drought, supporting the optimal partitioning theory. The biomass fractions of Biyu did not change as much as Xiaoye, and, more importantly, the standardized major axis analysis between leaf, stem and root in Biyu showed significant linear relationships, supporting allometric partitioning theory (Figures 1 and 2). Thus, Xiaoye showed flexible biomass partitioning among organs to optimize water, carbon and nitrogen balances, which could enhance acclimation to the low water availability but high sunlight conditions in semi-arid areas. The different biomass allocation patterns of Biyu and Xiaoye may indicate the tradeoff between the maximum biomass under optimal conditions and the ability to produce stable biomass over different environmental factors proposed by Weiner et al. [26].

The two clones also showed different leaf ecophysiological traits under soil water and nitrogen availabilities. Drought significantly increased the MDA and NPQ in Biyu but not in Xiaoye, and lower POD and SOD activities in Xiaoye suggest more stable oxidant content than that in Biyu. This could mean that membrane systems were significantly damaged by drought in Biyu. The decline of Φ_{PSII} and A_{sat} in Biyu under drought supports this, verifying that Biyu has lower drought resistance than Xiaoye [16,17]. Nitrogen addition totally or partly mitigated the membrane system damages and improved photosynthesis and growth both in Biyu and Xiaoye seedlings. For Biyu seedlings, a larger single leaf area,

LMA and LD may contribute to a larger leaf biomass allocation, while Xiaoye seedlings showed stable leaf ecophysiological traits. Furthermore, it seems that Biyu had soluble sugars as the main osmotic regulator in leaves, while in Xiaoye, it was free proline.

The results of PCA analysis showed that NR_{leaf} and NR_{root} were two major contributors to the differentiation between the clones (Figure 6). The partitioning of nitrate assimilation between shoot and root is plastic and influenced by nitrogen types and availability, plant species, air temperature, air CO_2 and abiotic stress [27]. However, the functional consequences of nitrate assimilation partitioning between shoot and root are still not clear.

We suggest that nitrate assimilation in leaves or/and in roots may influence biomass allocation patterns and thus partly explain differences between the clones. Nitrate and ammonium are two main inorganic nitrogen sources for poplars, and assimilation depends on species and soil properties [28]. After being absorbed by transporters in the root epidermal cell membrane, nitrate ions are reduced to ammonium in roots by NR and nitrite reductase (NiR). Ammonium ions are then added to carbon skeletons to produce amino acids via the glutamine synthetase (GS) and glutamate synthase or glutamate-2-oxoglutarate aminotransferase (GOGAT) cycle [29]. In roots, these enzymes consume energy from glycolysis and the oxidative pentose phosphate pathway, while nitrate assimilation in leaves may also be based on photosynthetic reductants [30]. Nitrate assimilation in leaves can consume the surplus ferredoxin, nicotinamide adenine dinucleotide phosphate (NADPH) and nicotinamide adenine dinucleotide (NADH) [31,32], which may contribute to a reduction in damages in photosynthetic structures caused by photooxidation during drought.

The results of the current study showed that both drought and the nitrogen addition increased NR_{leaf} in Biyu and Xiaoye seedlings (Figure 3). Increased NR_{leaf} during drought could be helpful to consume excess photochemical energy and to maintain chloroplast stability (Figure 7). Nitrate assimilation in leaves could also generate higher osmotic potential through nitrate, potassium and malate accumulation to improve leaf expansion, compared with nitrate assimilation in roots [27]. This may explain the alleviation of leaf ecophysiological traits and the growth of the two clones by nitrogen addition under drought. Improved leaf nitrogen assimilation under high nitrogen availability can also provide the protein basis for the enhancement of the antioxidant enzyme activity, repairing and renewing chlorophyll, and accumulation of free proline, consistent with what Shi et al. [33] found in *Catalpa bungei*. Lower NR_{leaf} in Biyu than Xiaoye may be one reason for its larger damages in chloroplast membrane and photosystem II under drought.

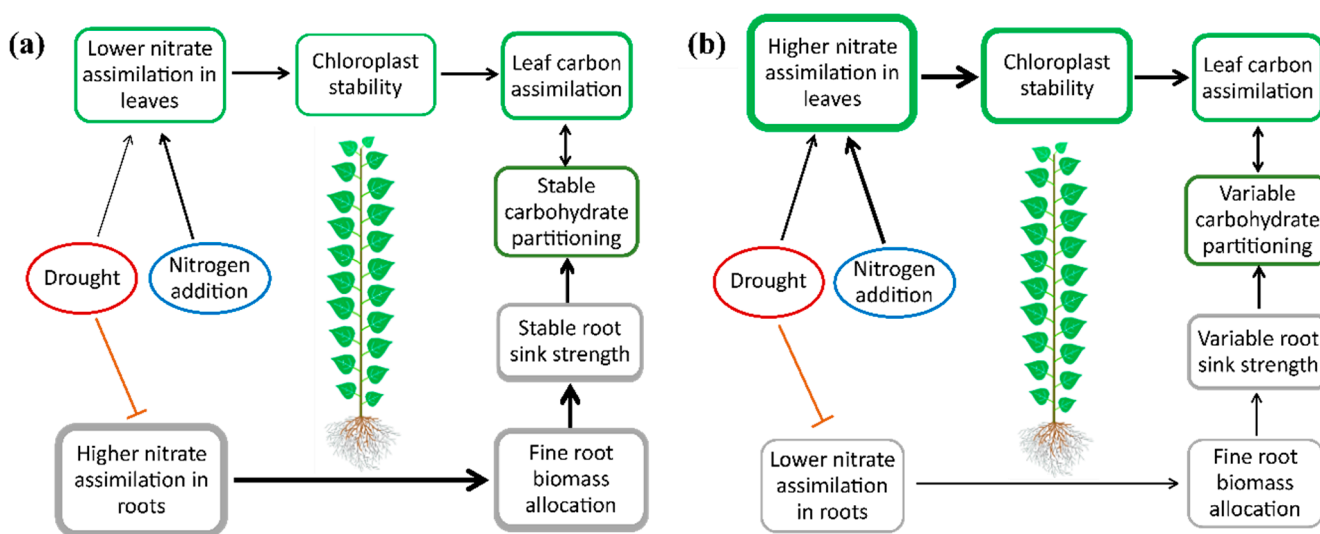


Figure 7. A schematic diagram proposing effects of nitrate assimilation in leaves and roots on biomass allocation in poplar seedlings: (a) depicts Biyu, following an allometric scaling model, while (b) depicts Xiaoye, following optimal partitioning theory. Black arrows indicate induction and orange T-lines indicate inhibition. Bold lines indicate strong effects or large pools.

Nitrate assimilation in roots requires a higher allocation of carbohydrates to roots than in leaves [27]. Thus, higher NR_{root} may contribute to the higher fine root biomass fraction in Biyu seedlings (Figure 1a; Supplementary Table S2). Because the leaf net photosynthetic rate could be inhibited by soluble sugar accumulation in leaves [34], the carbohydrate demand in fine roots could enhance the sink strength and stimulate carbohydrate exportation and maintain a high carbon assimilation in leaves, resulting in a large whole-plant biomass under high water and nitrogen availability (Figure 1a and Figure 7). However, NR is rapidly turned over and has complex regulatory mechanisms [32]. Additional experiments on NR regulation in poplars under water and nitrogen availabilities are needed to understand the influence of nitrate assimilation on biomass allocation, for example, by studies of nitrogen metabolism in additional clones of *Populus*.

5. Conclusions

Two poplar clones under water and nitrogen availabilities showed different biomass allocation patterns. Biyu followed allometric partitioning theory, and Xiaoye supported optimal partitioning theory. The two clones differed in nitrate reductase activity, with Biyu having the higher activity in roots, while Xiaoye had the higher activity in leaves. Furthermore, the two clones differed in drought stress response and in reaction to nitrogen fertilization, with Xiaoye being the least affected by both. We suggest that the place of nitrate assimilation may partly explain why plants follow different biomass allocation strategies, but this hypothesis needs to be examined by additional studies.

Supplementary Materials: The following supporting information can be downloaded at <https://www.mdpi.com/article/10.3390/f15050779/s1>, Figure S1: Peroxidase (POD) and superoxide dismutase (SOD) activity changes in leaves of Biyu and Xiaoye; Table S1: Plant height and base diameter changes after 106 days of water and/or nitrogen availability treatments for Biyu and Xiaoye seedlings; Table S2: The significance levels of clone, water, nitrogen and their interactions in biomass distribution of Biyu and Xiaoye seedlings.

Author Contributions: Conceptualization, W.W. and J.S.; methodology, W.W., J.S., T.G. and Q.X.; formal analysis, W.W.; investigation, J.S., T.G. and Q.X.; resources, W.W.; data curation, J.S.; writing—original draft preparation, W.W.; writing—review and editing, A.R.; funding acquisition, W.W. All authors have read and agreed to the published version of the manuscript.

Funding: This study was funded by the National Natural Science Foundation of China, grant number 31400527; the Applied Basic Research Project of Shanxi Province, grant number 201701D221190; China Scholarship Council, grant number 202108140068; the Startup Foundation for Introducing Talent of SXAU, grant number 2013YJ18; and the Science and Technology Innovation Foundation of SXAU, grant number 2014001.

Data Availability Statement: The data are available from the corresponding author upon reasonable request.

Acknowledgments: We thank Lisbeth G. Thygesen at the University of Copenhagen for her insightful suggestions.

Conflicts of Interest: The authors declare no conflicts of interest.

References

1. Weiner, J. Allocation, plasticity and allometry in plants. *Perspect. Plant Ecol. Evol. Syst.* **2004**, *6*, 207–215. [[CrossRef](#)]
2. Poorter, H.; Niklas, K.J.; Reich, P.B.; Oleksyn, J.; Poot, P.; Mommer, L. Biomass allocation to leaves, stems and roots: Meta-analyses of interspecific variation and environmental control. *New Phytol.* **2012**, *193*, 30–50. [[CrossRef](#)] [[PubMed](#)]
3. Liu, R.; Yang, X.; Gao, R.; Hou, X.; Huo, L.; Huang, Z.; Cornelissen, J.H.C. Allometry rather than abiotic drivers explains biomass allocation among leaves, stems and roots of *Artemisia* across a large environmental gradient in China. *J. Ecol.* **2021**, *109*, 1026–1040. [[CrossRef](#)]
4. Ågren, G.I.; Ingestad, T. Root: Shoot ratio as a balance between nitrogen productivity and photosynthesis. *Plant Cell Environ.* **1987**, *10*, 579–586. [[CrossRef](#)]

5. Feng, H.; Guo, J.; Peng, C.; Kneeshaw, D.; Roberge, G.; Pan, C.; Ma, X.; Zhou, D.; Wang, W. Nitrogen addition promotes terrestrial plants to allocate more biomass to aboveground organs: A global meta-analysis. *Global Chang. Biol.* **2023**, *29*, 3970–3989. [[CrossRef](#)] [[PubMed](#)]
6. McDowell, N.; Pockman, W.T.; Allen, C.D.; Breshears, D.D.; Cobb, N.; Kolb, T.; Plaut, J.; Sperry, J.; West, A.; Williams, D.G.; et al. Mechanisms of plant survival and mortality during drought: Why do some plants survive while others succumb to drought? *New Phytol.* **2008**, *178*, 719–739. [[CrossRef](#)] [[PubMed](#)]
7. Thornley, J.H.M. A balanced quantitative model for root: Shoot ratios in vegetative plants. *Ann. Bot.* **1972**, *36*, 431–441. [[CrossRef](#)]
8. Müller, I.; Schmid, B.; Weiner, J. The effect of nutrient availability on biomass allocation patterns in 27 species of herbaceous plants. *Perspect. Plant Ecol. Evol. Syst.* **2000**, *3*, 115–127. [[CrossRef](#)]
9. Coleman, J.S.; McConnaughay, K.D.M.; Ackerly, D.D. Interpreting phenotypic variation in plants. *Trends Ecol. Evol.* **1994**, *9*, 187–191. [[CrossRef](#)]
10. Niklas, K.J.; Enquist, B.J. Canonical rules for plant organ biomass partitioning and annual allocation. *Am. J. Bot.* **2002**, *89*, 812–819. [[CrossRef](#)]
11. Enquist, B.J.; Niklas, K.J. Global allocation rules for patterns of biomass partitioning in seed plants. *Science* **2002**, *295*, 1517–1520. [[CrossRef](#)]
12. Smith-Martin, C.M.; Xu, X.; Medvigy, D.; Schnitzer, S.A.; Powers, J.S. Allometric scaling laws linking biomass and rooting depth vary across ontogeny and functional groups in tropical dry forest lianas and trees. *New Phytol.* **2019**, *226*, 639–640. [[CrossRef](#)] [[PubMed](#)]
13. Poorter, H.; Jagodzinski, A.M.; Ruiz-Peinado, R.; Kuyah, S.; Luo, Y.; Oleksyn, J.; Usoltsev, V.A.; Buckley, T.N.; Reich, P.B.; Sack, L. How does biomass distribution change with size and differ among species? An analysis for 1200 plant species from five continents. *New Phytol.* **2015**, *208*, 736–749. [[CrossRef](#)] [[PubMed](#)]
14. Robinson, D. OPT-ing out: Root–shoot dynamics are caused by local resource capture and biomass allocation, not optimal partitioning. *Plant Cell Environ.* **2023**, *46*, 3023–3039. [[CrossRef](#)] [[PubMed](#)]
15. Puglielli, G.; Laanisto, L.; Poorter, H.; Niinemets, Ü. Global patterns of biomass allocation in woody species with different tolerances of shade and drought: Evidence for multiple strategies. *New Phytol.* **2021**, *229*, 308–322. [[CrossRef](#)] [[PubMed](#)]
16. Shang, J.; Zhao, Y.; Wang, W.; Gao, T.; Zong, Y. Response of drought on water and nitrogen utilization and carbohydrate distribution of *Populus × euramericana* ‘Biyu’ cuttings. *Arid Zone Res.* **2022**, *39*, 893–899.
17. Gao, T.; Shang, J.; Song, L.; Wang, W. Responses of leaf photosynthetic and anatomical characteristics in *Populus simonii* cuttings to drought and re-watering. *Sci. Soil Water Conserv.* **2021**, *19*, 18–26.
18. Fahrenkrog, A.M.; Neves, L.G.; Resende Jr, M.F.R.; Dervinis, C.; Davenport, R.; Barbazuk, W.B.; Kirst, M. Population genomics of the eastern cottonwood (*Populus deltoides*). *Ecol. Evol.* **2017**, *7*, 9426–9440. [[CrossRef](#)] [[PubMed](#)]
19. Wei, Z.Z.; Zhao, X.; Pan, W.; Zhang, J.F.; Li, B.L.; Zhang, D.Q. Phenotypic variation among five provenances of *Populus simonii* in northern China. *For. Stud. China* **2011**, *13*, 97–103. [[CrossRef](#)]
20. Murchie, E.H.; Lawson, T. Chlorophyll fluorescence analysis: A guide to good practice and understanding some new applications. *J. Exp. Bot.* **2013**, *64*, 3983–3998. [[CrossRef](#)]
21. Minocha, R.; Martinez, G.; Lyons, B.; Long, S. Development of a standardized methodology for quantifying total chlorophyll and carotenoids from foliage of hardwood and conifer tree species. *Can. J. For. Res.* **2009**, *39*, 849–861. [[CrossRef](#)]
22. Sáez-Plaza, P.; Navas, M.J.; Wybraniec, S.; Michałowski, T.; Asuero, A.G. An overview of the kjeldahl method of nitrogen determination. Part II. sample preparation, working scale, instrumental finish, and quality control. *Crit. Rev. Anal. Chem.* **2013**, *43*, 224–272. [[CrossRef](#)]
23. Hodges, D.M.; DeLong, J.M.; Forney, C.F.; Prange, R.K. Improving the thiobarbituric acid-reactive-substances assay for estimating lipid peroxidation in plant tissues containing anthocyanin and other interfering compounds. *Planta* **1999**, *207*, 604–611. [[CrossRef](#)]
24. Landhäusser, S.M.; Chow, P.S.; Dickman, L.T.; Furze, M.E.; Kuhlman, I.; Schmid, S.; Wiesenbauer, J.; Wild, B.; Gleixner, G.; Hartmann, H.; et al. Standardized protocols and procedures can precisely and accurately quantify non-structural carbohydrates. *Tree Physiol.* **2018**, *38*, 1764–1778. [[CrossRef](#)] [[PubMed](#)]
25. R Core Team. R: A Language and Environment for Statistical Computing. Available online: <https://www.R-project.org> (accessed on 16 June 2023).
26. Weiner, J.; Du, Y.-L.; Zhao, Y.-M.; Li, F.-M. Allometry and yield stability of cereals. *Front. Plant Sci.* **2021**, *12*, 681490. [[CrossRef](#)] [[PubMed](#)]
27. Andrews, M.; Raven, J.A. Root or shoot nitrate assimilation in terrestrial vascular plants—Does it matter? *Plant Soil* **2022**, *476*, 31–62. [[CrossRef](#)]
28. Rennenberg, H.; Wildhagen, H.; Ehling, B. Nitrogen nutrition of poplar trees. *Plant Biol.* **2010**, *12*, 275–291. [[CrossRef](#)]
29. Miller, A.J.; Cramer, M.D. Root nitrogen acquisition and assimilation. *Plant Soil* **2005**, *274*, 1–36. [[CrossRef](#)]
30. Andrews, M. The partitioning of nitrate assimilation between root and shoot of higher plants. *Plant Cell Environ.* **1986**, *9*, 511–519. [[CrossRef](#)]
31. Xu, G.; Fan, X.; Miller, A.J. Plant nitrogen assimilation and use efficiency. *Annu. Rev. Plant Biol.* **2012**, *63*, 153–182. [[CrossRef](#)]
32. Campbell, W.H. Nitrate reductase structure, function and regulation: Bridging the gap between biochemistry and physiology. *Annu. Rev. Plant Physiol. Plant Mol. Biol.* **1999**, *50*, 277–303. [[CrossRef](#)]

33. Shi, H.; Ma, W.; Song, J.; Lu, M.; Rahman, S.U.; Bui, T.T.X.; Vu, D.D.; Zheng, H.; Wang, J.; Zhang, Y. Physiological and transcriptional responses of *Catalpa bungei* to drought stress under sufficient- and deficient-nitrogen conditions. *Tree Physiol.* **2017**, *37*, 1457–1468. [[CrossRef](#)] [[PubMed](#)]
34. Goldschmidt, E.E.; Huber, S.C. Regulation of photosynthesis by end-product accumulation in leaves of plants storing starch, sucrose, and hexose sugars. *Plant Physiol.* **1992**, *99*, 1443–1448. [[CrossRef](#)] [[PubMed](#)]

Disclaimer/Publisher’s Note: The statements, opinions and data contained in all publications are solely those of the individual author(s) and contributor(s) and not of MDPI and/or the editor(s). MDPI and/or the editor(s) disclaim responsibility for any injury to people or property resulting from any ideas, methods, instructions or products referred to in the content.